Sound wave propagation in armchair single walled carbon nanotubes under thermal environment

Mokhtar Naceri,[1] Mohamed Zidour,[2,3] Abdelwahed Semmah,[1]
Mohammed Sid Ahmed Houari,[2,4] Abdelnour Benzair,[1] and Abdelouahed Tounsi[2,a)]
[1]*Université de Sidi Bel Abbés, Département de physique, BP 89 Cité Ben M'hidi, 22000 Sidi Bel Abbés, Algeria*
[2]*Laboratoire des Matériaux et Hydrologie, Université de Sidi Bel Abbés, BP 89 Cité Ben M'hidi, 22000 Sidi Bel Abbés, Algeria*
[3]*Université Ibn Khaldoun, BP 78 Zaaroura, 14000 Tiaret, Algeria*
[4]*Département de génie civil, Université de Mascaraa, Algeria*

(Received 12 September 2011; accepted 19 November 2011; published online 28 December 2011)

This paper develops a model that analyzes the wave propagation in armchair single-walled carbon nanotubes (SWCNTs) under thermal environment. The effect of a small length scale is incorporated in the formulations using nonlocal Levinson beam model. Unlike Timoshenko beam theory, Levinson beam theory satisfies zero traction boundary conditions on the upper and lower surface of the structures, so there is no need to use a shear correction factor. The equivalent Young's modulus and shear modulus for armchair SWCNT are derived using an energy-equivalent model. Results indicate significant dependence of natural frequencies on the temperature change as well as the chirality of armchair carbon nanotube. These findings are important in mechanical design considerations of devices that use carbon nanotubes. © *2011 American Institute of Physics*. [doi:10.1063/1.3671636]

I. INTRODUCTION

After the discovery of carbon nanotube by Iijima,[1] a new era has been evolved in the field of nano science and technology. Carbon nanotube is popular among researchers due to its small size, unique atomic arrangement of carbons, and outstanding mechanical, electrical, and physical properties.[2] The molecular simulation[3–5] or atomic models are accurate in nanostructure analysis due to the growth of supercomputer and cluster technology. But the computational cost and time are not affordable for various practical applications. The general classical continuum model does not account for nonlocal effects. The nonlocal continuum theory was proposed by Eringen[6] for the analysis of nanotube as an alternative method for molecular dynamic simulation. According to the nonlocal theory, the stresses at any point in an elastic continuum are not only depending on the strain at the same point but also the strains from all other points in the body. Implementation of nonlocal continuum model and the relevant computational work is easy and convenient.[7–16] Using continuum model and nonlocal elasticity theory, various researchers[7–13] have successfully studied the small scale effects of carbon nanotube.

The vibration and buckling studies of carbon nanotube are carried out using nonlocal Euler-Bernoulli beam theory.[14–18] The effect of shear deformation and rotary inertia is neglected in these analyses. The nonlocal Timoshenko beam models are used to analyze the vibration and buckling behavior of carbon nanotube with shear deformation effects.[19–23] More recently, Murmu and Adhikari[24] have analyzed the longitudinal vibration of double nanorod systems using the nonlocal elasticity. Murmu and Adhikari[25,26] have developed a nonlocal double-elastic beam model and applied it to investigate the small scale effect on the free vibration and the axial instability of the double-nanobeam system. Şimşek[27] studied the dynamic behavior of a single-walled carbon nanotube subjected to a moving harmonic load based on Eringen's nonlocal elasticity theory. Recently, Şimşek[28] presents a unique simple method of obtaining the exact solution based on the nonlocal Euler–Bernoulli beam theory for the forced vibration of an elastically connected double-carbon nanotube system (DCNTS) carrying a moving nanoparticle. The classical beam theory of Euler–Bernoulli has been used to study the dynamic and static behaviors of CNTs to show that classical theory is adequate for large aspect (length-to-diameter) ratios. Şimşek[29] performed the dynamic analysis of an embedded single-walled carbon nanotube traversed by a moving nanoparticle based on the nonlocal Timoshenko beam theory, including transverse shear deformation and rotary inertia. However, Timoshenko beam theory does not satisfy zero shear stress conditions on the upper and lower surface of structures. A shear correction factor, which is changing from structure to structure, used to satisfy upper and lower surface boundary conditions. This draw back of Timoshenko beam theory is solved by some higher order shear deformation theories, such as the Levinson beam theory.[30,31]

Although several studies on the nonlocal dynamic behavior and wave propagation in carbon nanotubes have been carried out based on beam model theory, no studies can be found for the nonlocal behavior of armchair CNTs based on the Levinson beam theory.[30,31] Therefore, the aim of this study is to analyze the wave propagation in armchair CNTs using nonlocal Levinson beam theory[30,31] including both the temperature change and the chirality of armchair carbon nanotube. The equivalent Young's modulus and shear modulus for armchair

a)Author to whom correspondence should be addressed. Electronic mail: tou_abdel@yahoo.com.

SWCNT are derived using an energy-equivalent model developed by Wu *et al.*[32] The obtained results in this paper can provide useful guidance for the study and design of the next generation of nanodevices that make use of the thermal vibration properties of armchair single-walled carbon nanotubes.

II. ATOMIC STRUCTURE OF CARBON NANOTUBE

Carbon nanotubes are considered to be tubes formed by rolling a graphene sheet a bout the $\vec{T}$ vector. A vector perpendicular to the $\vec{T}$ is the chiral vector denoted by $\vec{C}_h$.

The chiral vector and the corresponding chiral angle define the type of CNT, i.e., zigzag, armchair, and chiral $\vec{C}_h$ can be expressed with respect to two base vectors $\vec{a}_1$ and $\vec{a}_2$ as under

$$\vec{C}_h = n\vec{a}_1 + m\vec{a}_2, \tag{1}$$

where n and m are the indices of translation, which decide the structure around the circumference. Figure 1 depicts the lattice indices of translation (n, m) along with the base vectors, $\vec{a}_1$ and $\vec{a}_2$. If the indices of translation are such that $m=0$ and $n=m$, then the corresponding CNTs are categorized as zigzag and armchair, respectively. Considering the chirality the diameter, the chiral angle of the CNT can be calculated by the chiral vector for each nanostructure.

The radius of the armchair nanotube in terms of the chiral vector components can be obtained from the relation[33]

$$R = \frac{3na}{2\pi}, \tag{2}$$

where a is the length of the carbon–carbon bond which is 1.42 Å.

Based on the link between molecular mechanics and solid mechanics, Wu *et al.*[32] developed an energy-equivalent model for studying the mechanical properties of SWCNTs. Using the same method, the equivalent Young's modulus and shear modulus of armchair nanotube are expressed as

$$E_a = \frac{4\sqrt{3}}{3}\frac{KC}{3Ct + 4Ka^2t(\lambda_{a1}^2 + 2\lambda_{a2}^2)},$$
$$G_a = \frac{6\sqrt{3}KC}{18Ct + Ka^2\lambda_a^2 t}, \tag{3}$$

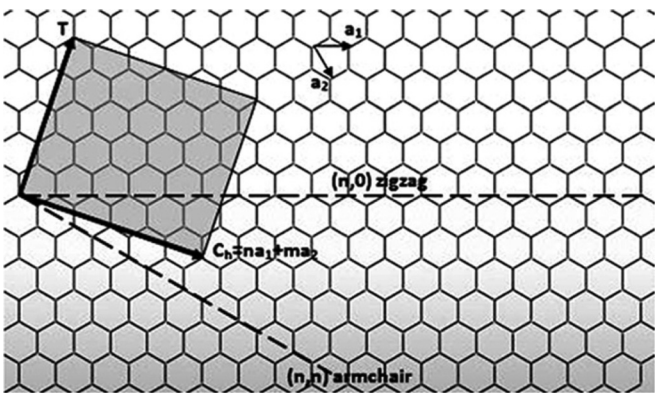

FIG. 1. Hexagonal lattice of graphene sheet including base vectors.

where K and C are the force constants, t is the thickness of the nanotube, and the parameters λ_{a1}, λ_{a2} and λ_a are given by

$$\lambda_{a1} = \frac{4 - \cos^2(\pi/2n)}{16 + 2\cos^2(\pi/2n)},$$
$$\lambda_{a2} = \frac{-\sqrt{12 - 3\cos^2(\pi/2n)}\cos^2(\pi/2n)}{32 + 4\cos^2(\pi/2n)}, \quad \text{and}$$
$$\lambda_a = \sqrt{4/\cos^2\frac{\pi}{2n} - 1}. \tag{4}$$

Letting $n \to \infty$, the expressions of Young's modulus and shear modulus of a graphite sheet is given by

$$E_g = \frac{8\sqrt{3}KC}{18Ct + Ka^2t}, \quad G_g = \frac{2\sqrt{3}KC}{(6C + Ka^2)t} \tag{5}$$

III. THE LEVINSON BEAM THEORY

In this section, derivation of the governing equations for the nanobeams is explained. Governing equations are derived for nanocomposite beams, and numerical results are given for anisotropic nanobeam. Consider a straight uniform composite beam having length L with thickness h. The beam is assumed to be constructed of arbitrary number, N, Therefore, the state of stress in kth layer accounting for transverse shear deformation and thermal effects is given by the generalized Hooke's law as follows[34]

$$\sigma_x^{(k)} = Q_{11}^{(k)}\left(\varepsilon_x - \alpha_x^{(k)}\Delta T\right), \quad \tau_{xz}^{(k)} = Q_{55}^{(k)}\gamma_{xz}, \tag{6}$$

where $Q_{ij}^{(k)}$ are well-known reduced stiffness[35] and k is the number of layers. ΔT is the temperature change during the thermal loading and $\alpha_x^{(k)}$ is the thermal expansion coefficient in the beam coordinate. Assuming that the deformations of the beam are in the x–z plane and denoting the displacement components along the x, y, and z directions by u_1, u_2, and u_3, respectively, the following displacement field for the beam is assumed on the basis of the Levinson beam theory:[30,31]

$$u_1 = u(x,t) + z\phi(x,t) - c_1 z^3\left(\phi + \frac{\partial w}{\partial x}\right), \quad u_2 = 0,$$
$$u_3 = w(x,t), \tag{7}$$

where $c_1 = 4/3h^2$ and h being the height of the beam. (u, w) are the axial and transverse displacements of the point $(x, 0)$ on the mid-plane (i.e., $z = 0$) of the beam. ϕ denotes the rotation of the cross-section.

The nonzero strains of the Levinson's beam theory are

$$\varepsilon_x = \varepsilon_x^0 + zk + z^3\eta, \quad \gamma_{xz} = \gamma + z^2\beta, \tag{8a}$$

With

$$k = \frac{\partial\phi}{\partial x}, \quad \eta = -c_1\left(\frac{\partial\phi}{\partial w} + \frac{\partial^2 w}{\partial x^2}\right), \quad \gamma = \left(\frac{\partial w}{\partial x} + \phi\right),$$
$$\beta = -c_2\left(\frac{\partial w}{\partial x} + \phi\right), \tag{8b}$$

where $c_2 = 4/h^2$.

The equations of Levinson's beam theory cannot be derived from the principle of total potential energy

$$\frac{\partial Q}{\partial x} - N_t \frac{\partial^2 w}{\partial x^2} = \rho A \frac{\partial^2 w}{\partial t^2}, \tag{9a}$$

$$\frac{\partial M}{\partial x} - Q = \rho I \frac{\partial^2 \phi}{\partial t^2}, \tag{9b}$$

where Q and M are the resultant shear force and the resultant bending moment on the cross-section, respectively. ρ is the mass density of the material, A is the area of the cross-section, and I is the moment of inertia of cross section of the beam. N_t is the axial force arising from the thermal effect and it is defined as

$$N_t = \alpha Q_{11} A \Delta T. \tag{10a}$$

IV. THE NONLOCAL LEVINSON BEAM MODEL OF ARMCHAIR SWCNT

Response of materials at the nanoscale is different from those of their bulk counter parts. Nonlocal elasticity is first considered by Eringen.[6] He assumed that the stress at a reference point is a functional of the strain field at every point of the continuum. Nonlocal stress tensor σ at point x' is defined by

$$\sigma = \int_V K(|x - x'|, \tau) S(x) dx, \tag{10b}$$

where $S(x')$ is the classical, macroscopic stress tensor at point x', $K(|x - x'|, \tau)$ is the kernel function, and τ is a material constant that depends on internal and external characteristic length (such as the lattice spacing and wavelength).

Nonlocal constitutive relations for present nanobeams can be written as

$$\sigma_x - \mu \frac{\partial^2 \sigma_x}{\partial x^2} = Q_{11} \varepsilon_x, \tag{11a}$$

$$\tau_{xz} - \mu \frac{\partial^2 \tau_{xz}}{\partial x^2} = Q_{55} \gamma_{xz}, \tag{11b}$$

where $\mu = (e_0 a)^2$ is nonlocal parameter, a is an internal characteristic length (e.g., length of C–C bond, lattice spacing, and granular distance), and e_0 is a constant. Choice of $e_0 a$ (in dimension of length) is crucial to ensure the validity of nonlocal models. This parameter was determined by matching the dispersion curves based on the atomic models.[6] For a specific material, the corresponding nonlocal parameter can be estimated by fitting the results of atomic lattice dynamic and experiment. Zhang *et al.*[36] gave a predicted value of e_0 and was approximated as 0.82 for a carbon nanotube. In the present result, this estimated value is used.

The stress resultants of the nonlocal Levinson beam theory are given by

$$M - \mu \frac{\partial^2 M}{\partial x^2} = D_{11} k + F_{11} \eta, \tag{12a}$$

$$Q - \mu \frac{\partial^2 Q}{\partial x^2} = A_{55} \gamma + H_{55} \beta, \tag{12b}$$

where

$$D_{11} = \int_{-h/2}^{h/2} Q_{11} z^2 dz, F_{11} = \int_{-h/2}^{h/2} Q_{11} z^4 dz,$$
$$A_{55} = \int_{-h/2}^{h/2} Q_{55} dz, \quad H_{55} = \int_{-h/2}^{h/2} Q_{55} z^2 dz \tag{12c}$$

The explicit expressions of the nonlocal bending moment M and the nonlocal shear force Q can be obtained by substituting Eqs. (9a) and (9b) into (12a) and (12b) as

$$M = D_{11} \frac{\partial \phi}{\partial x} - c_1 F_{11} \left(\frac{\partial \phi}{\partial x} + \frac{\partial^2 w}{\partial x^2} \right) + \mu \left(N_t \frac{\partial^2 w}{\partial x^2} + \rho A \frac{\partial^2 w}{\partial t^2} + \rho I \frac{\partial^3 \phi}{\partial x \partial t^2} \right), \tag{13a}$$

$$Q = K_{55} \left(\phi + \frac{\partial w}{\partial x} \right) + \mu \left(N_t \frac{\partial^3 w}{\partial x^3} + \rho A \frac{\partial^3 w}{\partial x \partial t^2} \right), \tag{13b}$$

where

$$K_{55} = (A_{55} - c_2 H_{55}) \tag{13c}$$

By substituting Eqs. (13a) and (13b) into (9a) and (9b), the equations of motion for the nonlocal Levinson beam model with thermal effect in displacement form can thus be obtained as

$$K_{55} \frac{\partial}{\partial x} \left(\phi + \frac{\partial w}{\partial x} \right) - N_t \frac{\partial^2}{\partial x^2} \left(w - \mu \frac{\partial^2 w}{\partial x^2} \right) = \rho A \frac{\partial^2}{\partial t^2} \left(w - \mu \frac{\partial^2 w}{\partial x^2} \right), \tag{14a}$$

$$D_{11} \frac{\partial^2 \phi}{\partial x^2} - c_1 F_{11} \left(\frac{\partial^2 \phi}{\partial x^2} + \frac{\partial^3 w}{\partial x^3} \right) - K_{55} \left(\phi + \frac{\partial w}{\partial x} \right) = \rho I \frac{\partial^2}{\partial t^2} \left(\phi - \mu \frac{\partial^2 \phi}{\partial x^2} \right). \tag{14b}$$

Since finding an analytical solution is possible for simply supported boundary conditions for the present problem, the SWNT beam is assumed simply supported. As a result, the boundary conditions have the following form:

$$w = 0 \quad \text{and} \quad M = 0 \quad \text{at} \quad x = 0, L \tag{15}$$

The following expansions of the generalized displacements w and ϕ satisfy the boundary conditions in Eq. (15)

$$w(x,t) = \sum_{k=1}^{\infty} W_k \sin \frac{k\pi x}{L} e^{i\omega_k t},$$
$$\phi(x,t) = \sum_{k=1}^{\infty} \Phi_k \cos \frac{k\pi x}{L} e^{i\omega_k t}. \tag{16}$$

Substitution of the expansions for w and ϕ from Eq. (16) into the equations of motion (14a) and (14b), we obtain

$$-\frac{k\pi}{L}K_{55}\left(\Phi_k+\frac{k\pi}{L}W_k\right)+\lambda_k N_t\left(\frac{k\pi}{L}\right)^2 W_k+\lambda_k\rho A\omega_k^2 W_k=0, \tag{17a}$$

$$-\left(\frac{k\pi}{L}\right)^2 D_{11}\Phi_k-\left[K_{55}-c_1F_{11}\left(\frac{k\pi}{L^2}\right)\right]\left(\Phi_k+\frac{k\pi}{L}W_k\right)+\lambda_k\rho I\omega_k^2\Phi_k=0, \tag{17b}$$

where

$$\lambda_k=1+\mu\left(\frac{k\pi}{L}\right)^2. \tag{17c}$$

Hence, the frequencies can be solved from Eqs. (17a) and (17b).

V. RESULTS AND DISCUSSIONS

Based on the formulations obtained above with the nonlocal Levinson beam model, the effect of the lattice indices of translation n on dynamic characteristics of armchair single-walled nanotubes in thermal environment are discussed here. The parameters used in calculations for the armchair SWCNTs are given as follows: the effective thickness of CNTs taken to be 0.258 nm,[32] the force constants[37] $K/2=46900$ kcal/mol/nm^2, and $C/2=63$ kcal/mol/rad^2, the mass density[22,23] $\rho=2.3$ g cm^{-3}.

Figure 2 shows the variation of Young's modulus with the structure characteristic of nanotube n. It can be seen that Young's modulus of armchair nanotubes increases with increasing the value n. For the shear modulus of carbon nanotubes, the same variation trend is present in Fig. 3.

From Figs. 2 and 3, it can be clearly observed that for carbon nanotubes with lattice index of translation n, Young's modulus and shear modulus exhibit a strong dependence on the structure characteristic of nanotube n. However for those with larger values of n, this dependence becomes very weak. The reason for this phenomenon is that a carbon nanotube

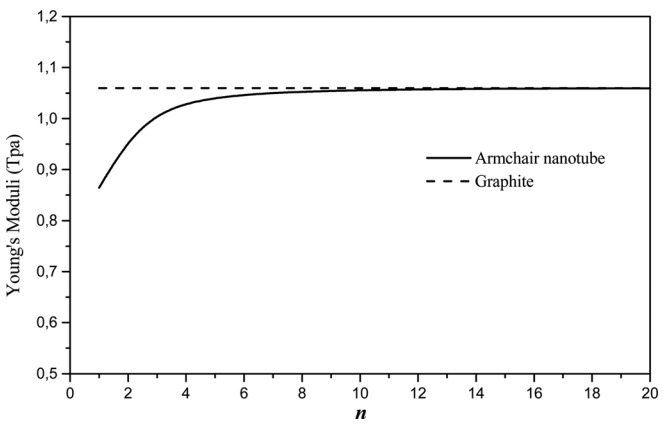

FIG. 2. The variation of Young's modulus.

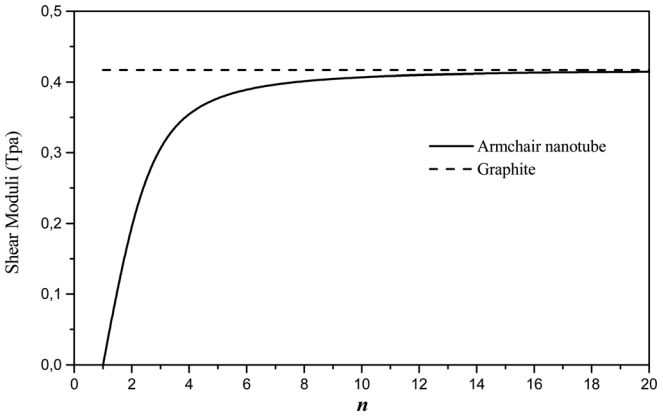

FIG. 3. The variation of shear modulus.

with smaller lattice indices of translation n has a larger curvature, which results in a more significant distortion of C–C bonds. As the structure characteristic of nanotube n increases, the effect of curvature diminishes gradually, and all of Young's modulus and shear modulus approach to the values of graphite sheet. This result has been also obtained and discussed by an earlier MD simulation.[38,39]

As indicated by Jiang *et al.*,[40] the coefficients of thermal expansion for CNTs are negative at lower temperature and become positive at higher temperature. Consequently, two cases of low temperature and high temperature are considered. For the case of room or low temperature, we suppose[22,41,42] $\alpha=-1.6\times10^{-6}$ K^{-1}, and for the case of high temperature, we suppose[22,41,42] $\alpha=1.1\times10^{-6}$ K^{-1}.

To investigate the effect of scale parameter and temperature change on vibrations of armchair SWCNTs, the results including and excluding the thermal effect and the nonlocal parameter are compared. In addition, the vibration characteristics of different armchair SWCNTs are compared in order to explore the effect of chirality. It follows that the ratios of the results with temperature change and nonlocal parameter to those without temperature change or nonlocal parameter are respectively given by

$$\chi_N=\frac{(\omega_k)_{NL}}{(\omega_k)_{LL}},\qquad \chi_{th}=\frac{(\omega_k)_{NL}}{(\omega_k)^0_{NL}} \tag{18}$$

where $(\omega_k)_{LL}$ is the frequency based on the local Levinson beam model including thermal effect and $(\omega_k)^0_{NL}$ is the frequency based on the nonlocal Levinson beam model without thermal effect ($\theta=0$).

Figures 4 to 7 show the dependence of the frequency ratios (χ_N) on the chirality of armchair carbon nanotube (n) for both cases of low and high temperatures. The frequency ratio χ_N serves as an index to assess quantitatively the scale effect on CNT vibration solution. It is clearly seen from Figs. 4 to 7 that for both cases of low and high temperatures, the frequency ratios (χ_N) are less than unity. This means that the application of the local Levinson beam model for CNT analysis would lead to an overprediction of the frequency if the scale effect between the individual carbon atoms in CNTs is neglected. The frequency ratios (χ_N) exhibit a dependence on the structure characteristic of armchair carbon

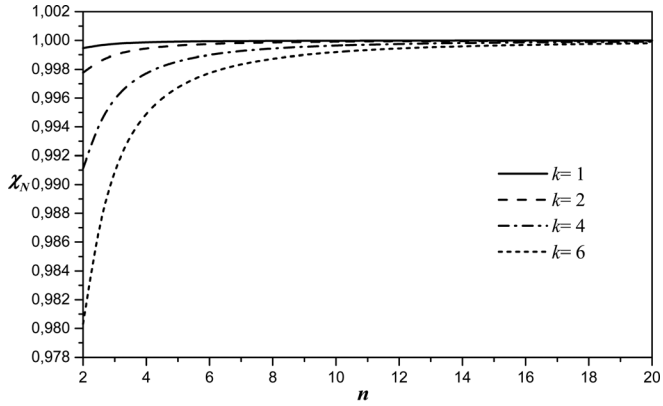

FIG. 4. Relationship between the values of ratio χ_N, chirality of armchair carbon nanotube n, and the vibrational mode number k in the case of low or room temperature ($\theta = 40$ K) and $L/d = 40$.

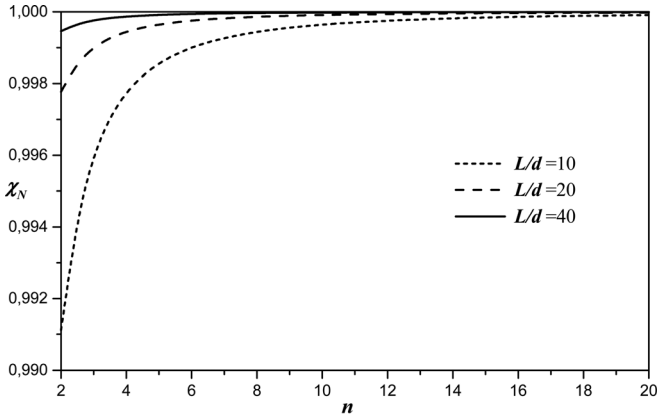

FIG. 6. Relationship between the values of ratio χ_N, chirality of armchair carbon nanotube n, and the aspect ratio L/d in the case of low or room temperature ($\theta = 40$ K) and $k = 1$.

nanotube n. However for armchair CNTs with larger values of n, this dependence becomes very weak. The reason for this phenomenon is that a carbon nanotube with smaller lattice indices of translation n has a larger curvature, which results in a more significant distortion of C–C bonds. Furthermore, the chirality of nanotube has not obvious effect on the ratio χ_N when the fundamental mode is considered.

It can be seen from Figs. 4 and 5 that the scale effect on the frequency ratios (χ_N) diminishes with increasing the index of translation (n) and becomes more significant with the increase of the vibrational mode k. However, the scale effect becomes less significant with the increase of the length-to-diameter ratio (L/d) as is shown in Figs. 6 and 7. Therefore, it is clear that the small scale effect is significant for short CNTs. It can be noted that for these types of CNTs (short CNTs), the transverse shear strain becomes important, and thus, the nonlocal Euler-Bernoulli beam theory cannot be used.

The effects of temperature change on the vibration frequencies for both cases of low and high temperatures are shown in Figs. 8 and 9 with the aspect ratio $L/d = 40$ and the vibrational mode $k = 1$. It can be seen that the frequency ratios (χ_{th}) vary linearly with the temperature change. In the case of room or low temperature (Fig. 8), the ratio χ_{th} increases monotonically as the temperature θ increases,

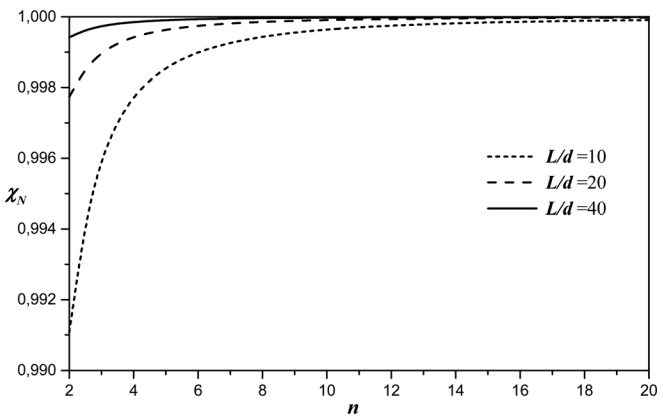

FIG. 7. Relationship between the values of ratio χ_N, chirality of armchair carbon nanotube n, and the aspect ratio L/d in the case of high temperature ($\theta = 40$ K) and $k = 1$.

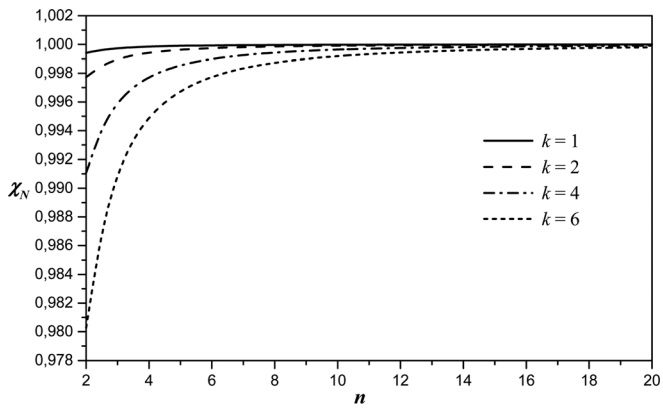

FIG. 5. Relationship between the values of ratio χ_N, chirality of armchair carbon nanotube n, and the vibrational mode number k in the case of high temperature ($\theta = 40$ K) and $L/d = 40$.

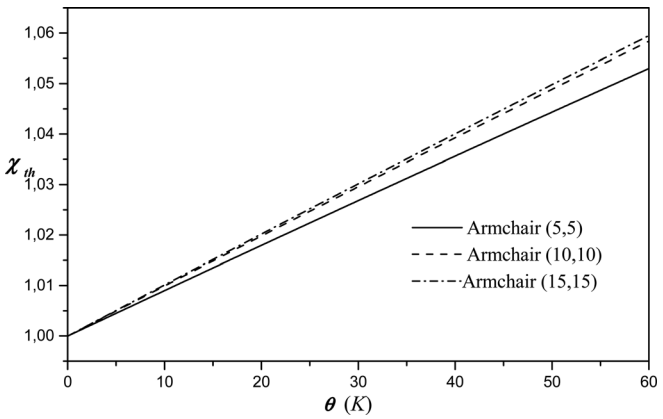

FIG. 8. Thermal effects on vibration frequencies for different armchair SWCNTs with the vibrational mode number $k = 1$ and $L/d = 40$ in the case of low or room temperature.

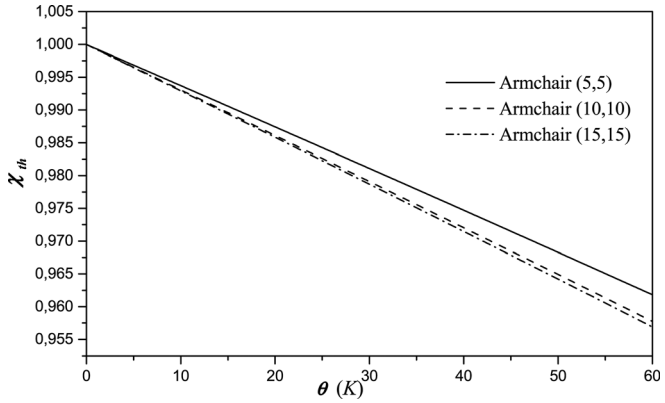

FIG. 9. Thermal effects on vibration frequencies for different armchair SWCNTs with the vibrational mode number $k = 1$ and $L/d = 40$ in the case of high temperature.

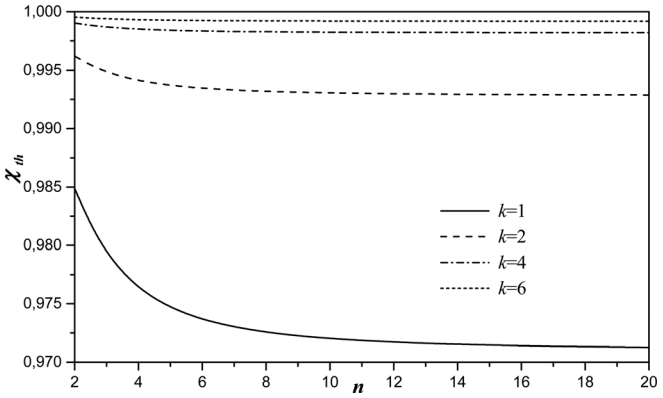

FIG. 11. Relationship between the values of ratio χ_{th}, chirality of armchair carbon nanotube n, and the vibrational mode number k in the case of the case of high temperature ($\theta = 40$ K) and $L/d = 40$.

indicating that the effect of temperature change leads to an increase of the fundamental frequency and especially for the armchair nanotubes with higher index of translation (n). For the case of high temperature, the thermal effects on the vibration frequencies are shown in Fig. 9. Contrary to the case of room or low temperature, it can be seen from Fig. 9 that the frequency ratios (χ_{th}) are less than unity. This means that the fundamental frequency diminishes with increasing the temperature change. In addition, an armchair nanotube with higher index of translation (n) will have the smallest fundamental frequency.

Figures 10 to 13 show the dependence of the frequency ratios (χ_{th}) on the chirality of armchair carbon nanotube (n) for both cases of low and high temperatures. With the aspect ratio $L/d = 40$ and the temperature change $\theta = 40$ K, the relationship among the ratio χ_{th}, the index of translation n, and the vibrational mode k is indicated in Figs. 10 and 11 for both cases of low and high temperatures, respectively. It can be seen that the chirality of nanotube has not obvious effect on the ratio χ_{th} for higher vibration modes. However, this effect becomes more significant for the fundamental mode. In addition, it can be observed that at low or room temperature the frequency ratio χ_{th} increases with the increase of the index of translation n, while at high temperature the ratio χ_{th} decreases with the increase of n.

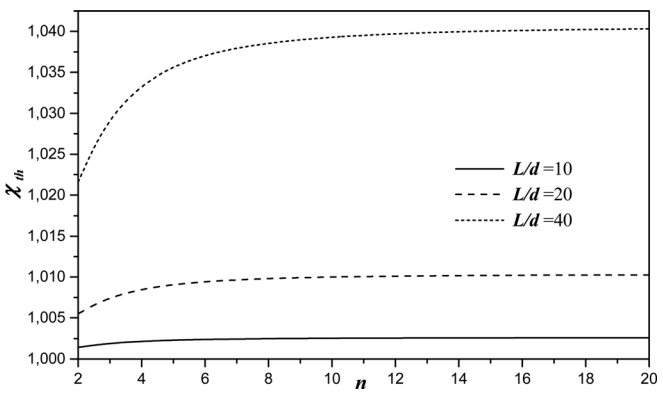

FIG. 12. Relationship between the values of ratio χ_{th}, chirality of armchair carbon nanotube n, and the aspect ratio L/d in the case of low or room temperature ($\theta = 40$ K) and $k = 1$.

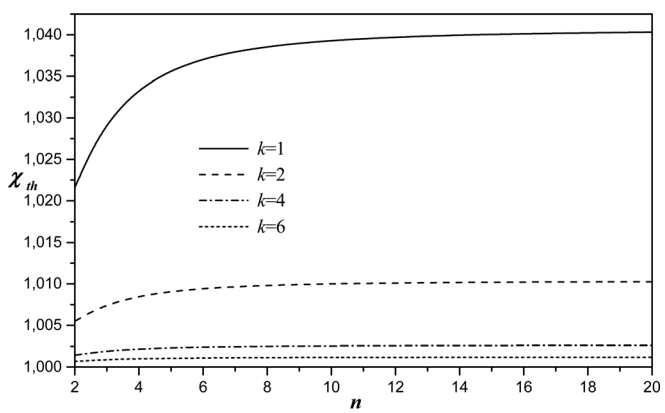

FIG. 10. Relationship between the values of ratio χ_{th}, chirality of armchair carbon nanotube n, and the vibrational mode number k in the case of low or room temperature ($\theta = 40$ K) and $L/d = 40$.

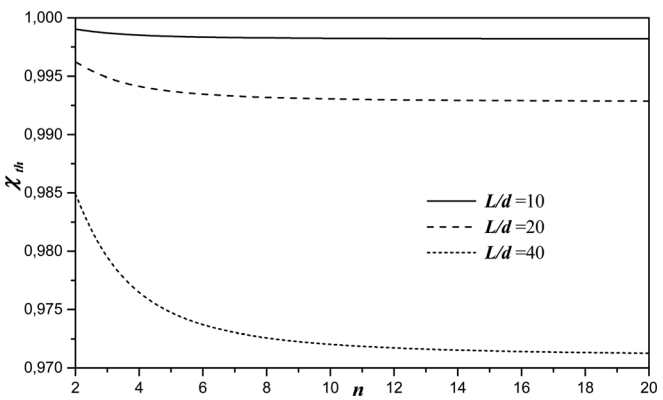

FIG. 13. Relationship between the values of ratio χ_{th}, chirality of armchair carbon nanotube n, and the aspect ratio L/d in the case of high temperature ($\theta = 40$ K) and $k = 1$.

With the vibrational mode number $k = 1$ and the temperature change $\theta = 40$ K, the relationship among the ratio χ_{th}, the index of translation n and the aspect ratio L/d is indicated in Figs. 12 and 13 for both cases of low and high temperatures, respectively. As can be seen, at low or room temperature the ratio χ_{th} increases with increasing the index of translation (n) and becomes more significant with the increase of the aspect ratio L/d, while at high temperature the ratio χ_{th} diminishes with the increase of n and the aspect ratio L/d. Hence, the chirality effect on the ratio χ_{th} is significant for slender CNTs.

VI. CONCLUSIONS

Thermal effect on the vibration characteristics of armchair SWCNTs is investigated in this paper based on the nonlocal Levinson beam theory. Theoretical formulations include the small scale effect, the temperature change and the chirality of armchair carbon nanotube. According to the study, the results showed the dependence of the vibration characteristics on the chirality of armchair carbon nanotube.

It is shown that the dynamical properties of the nanotubes based on the classical Levinson beam theory are over estimated. Hence, the work in the manuscript not only reveals the significance of the small-scale effect and the chirality effect on CNTs mechanical response but also points out the limitation of the applicability and feasibility of local continuum models in analysis of CNTs mechanical behaviors. The thermal effect on the frequencies decreases with the increase of the vibrational mode number k and increase with increasing the aspect ratio L/d, the index of translation n, and temperature change θ. It is also shown that the values of the frequencies accounting for the thermal effect are larger than those ignoring the influence of temperature change for the case of room or low temperature, whereas the values of ω_k with the thermal effect are smaller than those excluding the thermal effect for the case of high temperature.

ACKNOWLEDGMENTS

This research was supported by the Algerian National Agency for Development of University Research (ANDRU) and University of Sidi Bel Abbes (UDL SBA) in Algeria.

[1] S. Iijima, Nature **354**, 56 (1991).
[2] E. W. Wong, P. E. Sheehan, and C. M. Lieber, Science **277**, 1971 (1997).
[3] B. I. Yakobson, C. J. Brabec, and J. Bernholc, Phys. Rev. Lett. **76**, 2511 (1996).
[4] C. F. Cornwell and L. T. Wille, Solid Stat. Commun. **101**, 555 (1997).
[5] N. Yao and V. Lordi, Phy. Rev. B **58**, 12649 (1998).
[6] A. C. Eringen, J. Appl. Phys. **54**, 4703 (1983).
[7] J. Peddieson, G. R. Buchanan, and R. P. McNitt, Int. J. Eng. Sci. **41**, 305 (2003).
[8] L. J. Sudak, J. Appl. Phys. **94**, 7281 (2003).
[9] Q. Wang and V. K. Varadan, Smart Mater. Struct. **14**, 281 (2005).
[10] Q. Wang, V. K. Varadan, and S. T. Quek, Phy. Lett. A **357**, 130 (2006).
[11] Q. Wang, G. Y. Zhou, and K. C. Lin, Int. J. Solids Struct. **43**, 6071 (2006).
[12] Q. Wang and K. M. Liew, Phy. Lett. A **363**, 236 (2007).
[13] P. Lu, H. P. Lee, C. Lu, and P. Q. Zhang, Int. J. Solids Struct. **44**, 5289 (2007).
[14] Y. Q. Zhang, G. R. Liu, and X. Y. Xie, Phys. Rev. B **71**, 195404 (2005).
[15] P. Lu, H. P. Lee, C. Lu, and P. Q. Zhang, J. Appl. Phys. **99**, 073510 (2006).
[16] M. Xu, Proc. R. Soc. A **462**, 2977 (2006).
[17] A. R. Setoodeh, M. Kosrownejad, and P. Malekzadeh, Physica E **43**, 1730 (2011).
[18] S. Narendar and S. Gopalakrishnan, Physica E **43**, 1185 (2011).
[19] Q. Wang and V. K. Varadhan, Smart Mater. Struct. **15**, 659 (2006).
[20] X. F. Li and B. L. Wang, Appl. Phys. Lett. **94**, 101903 (2009).
[21] J. N. Reddy and S. D. Pang, J. Appl. Phys. **103**, 023511 (2008).
[22] A. Benzair, A. Tounsi, A. Besseghier, H. Heireche, N. Moulay, and L. Boumia, J. Phys. D. **41**, 225404 (2008).
[23] H. Heireche, A. Tounsi, A. Benzair, M. Maachou, and E. A. Adda Bedia, Physica E **40**, 27911 (2008).
[24] T. Murmu and S. Adhikari, Physica E **43**, 415 (2010).
[25] T. Murmu and S. Adhikari, J. Appl. Phys. **108**, 083514 (2010).
[26] T. Murmu and S. Adhikari, Phys. Lett. A **375**, 601 (2011).
[27] M. Şimşek, Physica E **43**, 182 (2010).
[28] M. Şimşek, Comput. Mater. Sci. **50**, 2112 (2011).
[29] M. Şimşek, Steel Compos. Struct. **11**, 59 (2011).
[30] M. Levinson, Mech. Res. Commun. **7**, 343 (1980).
[31] M. Levinson, J. Sound Vib. **74**, 81 (1981).
[32] Y. Wu, X. Zhang, A. Y. T. Leung, and W. Zhong, Thin-Walled Struct. **44**, 667 (2006).
[33] Y. Tokio, Synth. Met. **70**, 1511 (1995).
[34] I. Mechab, A. Tounsi, M. A. Benatta, and E. A. Adda bedia, J. Math. Anal. Appl. **346**, 468 (2008).
[35] C. T. Herakovich, *Mechanics of Fibrous Composites* (Wiley, New York, 1998).
[36] Y. Q. Zhang, G. R. Liu, and X. Y. Xie, Phys. Rev. B. **71**, 195404 (2005).
[37] W. D. Cornell, P. Cieplak, C. I. Bayly, I. R. Gould, K. M. Merz, Jr., D. M. Ferguson, D. C. Spellmeyer, T. Fox, J. W. Caldwell, and P. A. Kollman, J. Am. Chem. Soc. **117**, (1995) 5179.
[38] B. I. Yakobson and P. H. Avour, in *Carbon Nanotubes*, edited by M. S. Dresselhaus and P. H. Avouris (Springer Verlag, Berlin-Heidelberg, 2001), Chap. 9, p. 287.
[39] V. N. Popov, V. E. Van Doren, and M. Balkanski, Phys. Rev. B **61**, 3078 (2000).
[40] H. Jiang, R. Liu, Y. Huang, and K. C. Hwang, J. Eng. Mater. Technol. **126**, 265 (2004).
[41] X. H. Yao and Q. Han, J. Eng. Mater. Technol. **128**, 419 (2006).
[42] X. H. Yao and Q. Han, Compos. Sci. Technol. **67**, 125 (2007).